

# Coined Quantum Walks on Complex Networks for Quantum Computers

Rei Sato\*

*Classiq Technologies G.K., 1-5-1 Marunouchi, Chiyoda-ku, Tokyo, 100-6509, Japan*

(Dated: December 19, 2025)

We propose a quantum circuit design for implementing coined quantum walks on complex networks. In complex networks, the coin and shift operators depend on the varying degrees of the nodes, which makes circuit construction more challenging than for regular graphs. To address this issue, we use a dual-register encoding. This approach enables a simplified shift operator and reduces the resource overhead compared to previous methods. We implement the circuit using Qmod, a high-level quantum programming language, and evaluated the performance through numerical simulations on Erdős–Rényi, Watts–Strogatz, and Barabási–Albert models. The results show that the circuit depth scales as approximately  $N^{1.9}$  regardless of the network topology. Furthermore, we execute the proposed circuits on the `ibm_torino` superconducting quantum processor for Watts–Strogatz models with  $N = 4$  and  $N = 8$ . The experiments show that hardware-aware optimization slightly improved the  $L_1$  distance for the larger graph, whereas connectivity constraints imposed overhead for the smaller one. These results indicate that while current NISQ devices are limited to small-scale validations, the polynomial scaling of our framework makes it suitable for larger-scale implementations in the early fault-tolerant quantum computing era.

Keywords: quantum walk, complex network

## I. INTRODUCTION

Quantum walks have emerged as one of the promising quantum gate-based algorithms for a wide range of potential use cases, including combinatorial optimization [1], financial modeling [2], and protein folding [3]. The quantum walks are known as the quantum counterparts of classical random walks and are broadly categorized into two models: continuous-time quantum walks (CTQWs) [4] and discrete-time quantum walks (DTQWs) [5]. While CTQWs describe graph dynamics through Hamiltonian evolution, DTQWs evolve via different unitary operators [6, 7]. In particular, the interplay between quantum walks and complex networks provides a variety of applications, including quantum search [4, 7, 8], network analysis [8–10], and quantum machine learning [11–13].

Research on the circuit implementation of quantum walks has made progress in recent years [14–26]. In the domain of the CTQWs, implementations have traditionally focused on regular structures such as complete graphs or hypercube lattices. However, recent works have begun to extend these frameworks to dynamics on complex networks [23–25]. Regarding the DTQWs, two primary approaches have been extensively studied. The first is Szegedy’s walk [6], which encodes quantum dynamics utilizing transition matrices derived from Markov chains. This model is inherently adaptable to general graphs and has been applied to various network algorithms [3, 10, 12]. In contrast, the second approach is the coined quantum walk [7]. The coined quantum walks have mainly focused on regular graph structures [17, 18, 21]. Although recent studies have explored coined walks on network structures [14, 15], these implementations are typically limited to specific topologies, such as star graphs or regular ring lattices. Consequently, establishing a systematic and resource-efficient circuit architecture

applicable to arbitrary complex networks remains an open challenge.

One of the major challenges in building quantum circuits for coined quantum walks on complex networks arises from their irregular structures, which require different coin and shift operators for each node. To address this issue, we previously proposed a circuit implementation that encodes the number of nodes and the maximum internal degree of freedom [27]. The required number of qubits is given by  $\lceil \log_2 N \rceil + \lceil \log_2 |E| \rceil$ . Moreover, the shift operator requires up to  $\lceil \log_2 |E| \rceil$  multi-controlled  $X$  (MCX) gates. This design poses a substantial resource overhead, particularly for dense or scale-free networks where the number of edges  $|E|$  significantly exceeds the number of nodes  $N$ , as seen in Watts–Strogatz [28], scale-free [29], and Erdős–Rényi [30] network models.

In this study, we propose a resource-efficient circuit design inspired by the construction techniques of Szegedy’s quantum walk to overcome these limitations. The coined walk in our approach is encoded using a dual-register quantum state representation, enabling a simplified shift operator based on SWAP gates. We implement the proposed architecture using Qmod [31], a high-level quantum programming language.

Our contribution lies in the development of a scalable and programmable circuit architecture suitable for practical deployment on near-term quantum computing platforms. We evaluate our framework across multiple classes of complex networks, including Erdős–Rényi random graphs [30], small-world networks [28], and scale-free networks [29]. Furthermore, to demonstrate the feasibility of our approach on real hardware, we executed the synthesized circuits on the `ibm_torino` superconducting quantum processor. We observed that applying hardware-aware compilation strategies resulted in slight improvements in circuit performance, suggesting that topology-aware circuit design will become increasingly important for implementing graph algorithms on near-term devices.

This paper is organized as follows. In Section II, we

\* Correspondence email address: rei@classiq.io

briefly explain three famous complex network models used for experiments. In Section III, we formulate the coined quantum walk model on complex networks. Section IV describes the circuit design and implementation strategy. Experimental results are presented in Section V. In Section VI, we discuss the broader implications of our findings. Finally, Section VII concludes the paper.

## II. COMPLEX NETWORK

We evaluate the proposed coined quantum walk circuit using three well-known complex network models, the Erdős–Rényi model [30], the Watts–Strogatz model [28], and the Barabási–Albert model [29]. Each of these models captures different structural characteristics found in real-world systems. We describe the generation procedure and define the relevant parameters for each model.

The Erdős–Rényi random graph  $G(N, p)$  is defined on  $N$  nodes, where each possible edge between distinct node pairs is independently included with probability  $p$  [30]. A graph containing  $M$  edges occurs with probability  $p^M(1-p)^{\binom{N}{2}-M}$ . The ER graph demonstrates that certain structural properties, such as connectivity, emerge sharply at critical probabilities—for instance, a graph becomes connected almost surely when  $p > \log N/N$ .

The Watts–Strogatz (WS) model  $G(N, k, \beta)$  generates small-world networks characterized by a high clustering coefficient and a short average path length that scales as  $L \sim \log N$  [28]. The model starts from a ring lattice in which each node is connected to its  $k$  nearest neighbors, and then each edge is rewired with probability  $\beta$ . As  $\beta$  increases from 0 to 1, the network transitions from a regular lattice to a random graph, retaining high clustering while achieving logarithmically short path lengths.

The Barabási–Albert (BA) model  $G(N, m)$  generates scale-free networks through a growth process governed by preferential attachment [29]. Starting from a small connected seed network, new nodes are added sequentially, and each new node connects to  $m$  existing nodes with a probability proportional to their current degree. As a result, the model produces networks whose degree distribution follows a power law,  $P(k) \sim k^{-\alpha}$ , where the exponent typically satisfies ( $\alpha \approx 3$ ).

## III. MATHEMATICAL MODEL

We describe a mathematical framework for coined discrete-time quantum walks on general undirected graphs, focusing on the definition of the Hilbert space, the coin operator, and the shift operator.

The complex network is represented as a graph  $G = (V, E)$ , where  $V = \{0, 1, 2, \dots, N - 1\}$  is the set of  $N$  nodes and  $E = \{e_{ij}\}$  is the set of edges. Fig. 1 shows an example of the quantum state of the quantum walker on node  $i$ . The quantum state of the

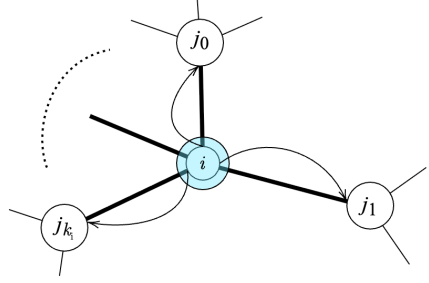


Figure 1. The definition of coined quantum walk on complex networks.  $j$  is the neighbor of node  $i$ .

walker at time step  $t$  is described as

$$|\psi(t)\rangle = \sum_{i \in V} \sum_{j \in \mathcal{N}(i)} \psi_{ij}(t) |i\rangle \otimes |i \rightarrow j\rangle, \quad (1)$$

where  $\mathcal{N}(i)$  denotes the set of neighbors of node  $i$ ,  $\psi_{ij}(t)$  denotes the probability amplitude of the walker moving from node  $i$  to node  $j$  and the basis state  $|i \rightarrow j\rangle$  also represents the direction from node  $i$  to node  $j$ .  $k_i$  is the number of links attached to node  $i$ .  $|\psi(t)\rangle$  is defined in the Hilbert space  $\bigoplus_{i=0}^{N-1} \mathcal{H}_i \otimes \mathcal{H}_{k_i}$ , where  $|i\rangle \in \mathcal{H}_i$  is associated with the positional degree of freedom, and  $|i \rightarrow j\rangle \in \mathcal{H}_{k_i}$  is associated with the internal degree of freedom.  $\psi_{ij}(t)$  is the probability amplitude of  $|i\rangle |i \rightarrow j\rangle$ .

The time evolution of the quantum walker is governed by alternating applications of the coin operator  $\hat{C}$  and the shift operator  $\hat{S}$ , as

$$|\psi(t)\rangle = [\hat{S}\hat{C}]^t |\psi(0)\rangle. \quad (2)$$

The initial state  $|\psi(0)\rangle$  is chosen as a uniform superposition over all nodes and their corresponding coin states:

$$|\psi(0)\rangle = \frac{1}{\sqrt{N}} \sum_{i \in V} \frac{1}{\sqrt{k_i}} \sum_{j \in \mathcal{N}(i)} |i\rangle \otimes |i \rightarrow j\rangle. \quad (3)$$

This choice of initial state ensures an unbiased exploration of the network, avoiding any preferential starting node or direction. The coin operator  $\hat{C}$  is position-dependent, as the degree  $k_i$  may vary for each node  $i$ . It is defined as  $\hat{C} = \sum_i |i\rangle \langle i| \otimes \hat{C}_i$ , where the coin operator  $\hat{C}_i$  at node  $i$  is given by

$$\hat{C}_i = 2 |s_i\rangle \langle s_i| - \hat{I}_i, \quad (4)$$

where  $|s_i\rangle = 1/\sqrt{k_i} \sum_{j \in \mathcal{N}(i)} |i \rightarrow j\rangle$ , and  $\hat{I}_i$  is the identity operator.

The shift operator  $\hat{S}$  moves the walker from the current node to its neighboring node and updates the internal coin state to indicate the new direction. It is defined as

$$\hat{S} |i\rangle |i \rightarrow j\rangle = |j\rangle |j \rightarrow i\rangle. \quad (5)$$

This type of shift operation, known as flip-flop shift, is particularly useful for handling networks with varying node degrees, as it naturally adapts to the graph's structure.

Finally, the probability of finding the walker at node  $i$  at time step  $t$  is given by

$$P_i(t) = \sum_{j=0}^{k_i-1} |(\langle i | \otimes \langle i \rightarrow j |) |\psi(t)\rangle|^2. \quad (6)$$

#### IV. CIRCUIT DESIGN

We propose a systematic method for building the quantum circuits to implement the quantum walks defined in Section III. We first encode the quantum state  $|i\rangle \otimes |i \rightarrow j\rangle$  using two quantum registers, both representing node labels.

$$|i\rangle \otimes |i \rightarrow j\rangle \rightarrow |i\rangle |j\rangle \quad (7)$$

The first and second registers are used for encoding the position degree and the inner degree of freedom of the quantum walker, respectively. The position state is defined by

$$\hat{U}_1 |0\rangle^n = \frac{1}{\sqrt{N}} \sum_{i=0}^{N-1} |i\rangle, \quad (8)$$

where  $i \in \{0, N-1\}$  is the  $i$ -th node label of the given graph with  $N$  nodes. The required qubit  $n$  is given by  $n = \lceil \log_2 N \rceil$ . The inner degree state is defined by

$$\hat{U}_2^{(i)} |0\rangle^n = \frac{1}{\sqrt{k_i}} \sum_{j=1}^N A_{i,j} |j\rangle, \quad (9)$$

where  $j \in \{0, N-1\}$  is the  $N$  dimensional vector and  $k_i$  is the degree of node  $i$ .  $A_{i,j}$  denotes the elements of the adjacency matrix of the given graph.  $A_{i,j} = 1$  if  $(i, j) \in E$ , and  $A_{i,j} = 0$  otherwise. We define the controlled operation  $C^n(\hat{U}_2)$  by the equation  $C^n(\hat{U}_2) |i\rangle |0\rangle^n = |i\rangle \hat{U}_2(i) |0\rangle^n$ , where  $\hat{U}_2(i)$  acts on the second register depending on the control state  $|i\rangle$ .

We can define the equal superposition state of the quantum walk on the complex network as

$$|\psi(0)\rangle = C^n(\hat{U}_2)(\hat{U}_1 \otimes \hat{I}) |0\rangle^n \otimes |0\rangle^n \quad (10)$$

$$= \frac{1}{\sqrt{N}} \sum_{i=0}^{N-1} |i\rangle \otimes \frac{1}{\sqrt{k_i}} \sum_{j=0}^{N-1} A_{i,j} |j\rangle. \quad (11)$$

The coin operator  $\hat{C}$  consists of controlled operation  $C^n(\hat{C}_i)$ . The coin operator  $\hat{C}_i$  based on the Eq. (4) is given by

$$\hat{C}_i = 2\hat{U}_2 |0\rangle^n \langle 0|^n \hat{U}_2^\dagger - \hat{I}^n. \quad (12)$$

The shift operator  $\hat{S}$  shifts the direction of the quantum walk by exchanging the two quantum registers. Since the quantum state is represented as  $|i\rangle \otimes |j\rangle$ , the shift operation is defined as

$$\hat{S} |i\rangle \otimes |j\rangle = |j\rangle \otimes |i\rangle. \quad (13)$$

This operation can be implemented by swapping each qubit of the first register with the corresponding qubit

of the second register using SWAP gates, realizing a flip-flop shift between adjacent nodes. The full register exchange can be realized by applying an  $n$ -qubit multi-SWAP operation that swaps all corresponding qubit pairs between the two registers.

As described in Eq. (2), one step consists of sequentially applying the coin operator  $\hat{C}$  followed by the shift operator  $\hat{S}$ . The circuit is composed of two main blocks: the coin operation blocks given and the shift operation block. By iteratively applying the unitary operation defined in Eq. (2), multiple steps of the quantum walk can be performed in a straightforward manner. Figure 2 illustrates the proposed quantum circuit for a single step of the coined quantum walk based on Eqs (8)-(13).

To create the quantum circuit, we use Qmod [31], a high-level language, and Synthesis [32], which automatically generates the circuit by allocating and optimizing available resources such as the number of qubits and the circuit depth. Synthesis also allows parameter tuning according to the desired circuit generation and optimization strategy. For our simple circuit evaluation, we set the parameters as `transpilation_option = AUTO_OPTIMIZE`, `debug_mode = False`, and `optimization_level = LIGHT`. See supplemental material for Qmod implementation.

#### V. RESULT

We first evaluated the proposed circuit for ER, WS, and BA models. For each network type, we generated graphs with node sizes  $N \in [10, 100]$ . We set parameters  $p$  as  $p = [0.2, 0.4, 0.6, 0.8, 1.0]$ ,  $\beta \in [0, 1]$ ,  $k = 4$ , and  $m \in [5, N-5]$  with increments of 5 for the ER model, WS model, and BA model, respectively. For each configuration, we generate three random instances and evaluate the average and standard deviation of the results to account for graph randomness.

We investigate the correctness of the proposed circuit by comparing the theoretical value for the small graphs. Fig. 3 shows the probability distribution of the quantum walk on the ER model with  $N = 10$  and  $p = 0.3$ . As a benchmark, the theoretical value is calculated using classical matrix-based simulation of the quantum walk dynamics. We confirm that the quantum circuit simulation results matched well with the theoretical values.

Figure 4(a) illustrates the scaling behavior of the proposed circuit depth with respect to the number of nodes in three complex network models. Across all three networks, the circuit depth consistently exhibited around  $N^\alpha$  ( $\alpha = 1.9$ ) growth as the number of nodes increased, given by  $D_{\text{ER}} = 38(12)N^{1.91(7)}$ ,  $D_{\text{WS}} = 41(8)N^{1.86(4)}$  and  $D_{\text{BA}} = 38(12)N^{1.90(7)}$  for ER, WS and BA models, respectively.

Figure 4(b) illustrates the scaling behavior of the proposed circuit depth with respect to the number of steps in three complex network models. Across all three network, the circuit depth given by  $D_{\text{ER}} = 8969(669)t^{0.86(1)}$ ,  $D_{\text{WS}} = 8841(743)t^{0.88(2)}$  and  $D_{\text{BA}} = 8841(743)t^{0.88(2)}$  for ER, WS and BA

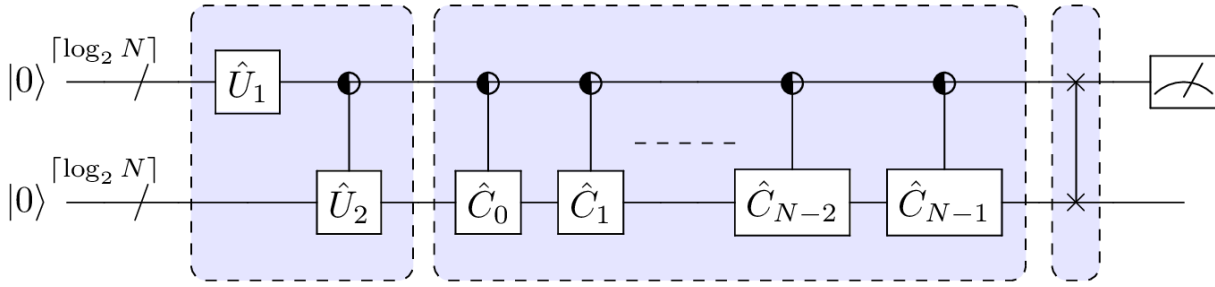


Figure 2. The quantum circuit for implementing the coined quantum walk on complex networks for the walker step as  $t = 1$ . The first dashed box from the left side represents the initial state of the quantum walker  $|\psi(0)\rangle$ . The half-filled circle denotes a control qubit based on its 0/1 binary state. The second dashed-box represents coin operator  $\hat{C} = \sum_i |i\rangle\langle i| \otimes \hat{C}_i$ . The third dashed box represents the swap operator as the shift operator  $\hat{S}$ .

	$N$	$ E $	$t = 1$	$t = 2$	$t = 3$	$t = 4$
$L_1^{\text{agn}}$	4	4	0.1742..	0.1326..	0.1237..	0.3126..
$L_1^{\text{hw}}$	4	4	0.2772..	0.1886..	0.1065..	0.3209..
Depth <sup>agn</sup>	4	4	820	1079	1408	1640
Depth <sup>hw</sup>	4	4	2397	3483	4354	5478
$L_1^{\text{agn}}$	8	16	0.2160..	0.2239..	0.08750..	0.2517..
$L_1^{\text{hw}}$	8	16	0.2050..	0.1949..	0.06796..	0.2280..
Depth <sup>agn</sup>	8	16	1427	1836	2357	2845
Depth <sup>hw</sup>	8	16	1396	1782	2344	8186

Table I. Experimental results on `ibm_torino`. We compare the total variation distance,  $L_1$ , and circuit depth between hardware-agnostic (agn) and hardware-aware (hw) synthesis approaches for different time steps  $t$ .

models, respectively.

This trend remained stable regardless of the specific structural parameters of the networks, such as the connection probability  $p$ , the rewiring probability  $\beta$ , or the attachment parameter  $m$ . The observed consistency across different models suggests that the proposed quantum circuit design is robust to topological variations in complex networks. This linear depth scaling is particularly important for near-term quantum computing, as circuit depth directly affects the feasibility of implementation on current quantum hardware. These results indicate that the proposed framework can reliably support a broad range of complex network structures without incurring significant additional complexity, thereby offering a scalable and generalizable approach to implementing coined quantum walks in quantum circuits.

Next, we validate the feasibility of our approach on actual quantum hardware. We executed the synthesized circuits on `ibm_torino`, a 133-qubit superconducting processor. We evaluate hardware performance using the total variation distance,  $L_1$  [33], defined as:

$$L_1(t) = \frac{1}{2} \sum_x |P_{\text{hw}}(t, x) - P_{\text{exact}}(t, x)|, \quad (14)$$

where  $P_{\text{hw}}(t, x)$  and  $P_{\text{exact}}(t, x)$  denote the probabil-

ity distributions obtained from the real hardware execution and the exact state-vector simulation, respectively.

To construct the quantum circuits for these experiments, we employed hardware-aware synthesis [34] to optimize circuits under specific hardware constraints and compare those circuits against a hardware-agnostic baseline.

Figure 5 shows the probability distributions of several time steps of the quantum walker. We conducted experiments on WS models with  $N = 4$  and  $N = 8$ . Although the experimental distributions exhibit quantitative deviations from the exact simulation due to noise inherent in current NISQ devices, distinct trends were observed regarding the synthesis strategy, as summarized in Table I. For the smaller WS model ( $N = 4$ ), the hardware-aware synthesis resulted in increased circuit depth and higher error rates compared to the agnostic approach. This indicates that for simple topologies, the routing overhead introduced by enforcing strict hardware constraints, such as SWAP gates for connectivity, can outweigh the benefits of optimization.

In contrast, for the larger WS model with  $N = 8$ , the hardware-aware synthesis demonstrated its efficacy. As shown in Table I, the hardware-aware circuits achieved reduced circuit depth and consistently lower  $L_1$  values compared to the agnostic baseline. These results highlight that as the graph size and circuit complexity increase, hardware-aware circuit design becomes crucial for mitigating noise and improving performance.

## VI. DISCUSSION

In this section, we discuss the scalability, resource efficiency, and hardware feasibility of the proposed circuit implementation.

The experimental results demonstrate that the circuit depth exhibits consistent scaling behavior with respect to the number of nodes for the three graph models. As shown in Fig. 4, the circuit depth scales as approximately  $N^{1.9}$  for ER, WS, and BA models. This

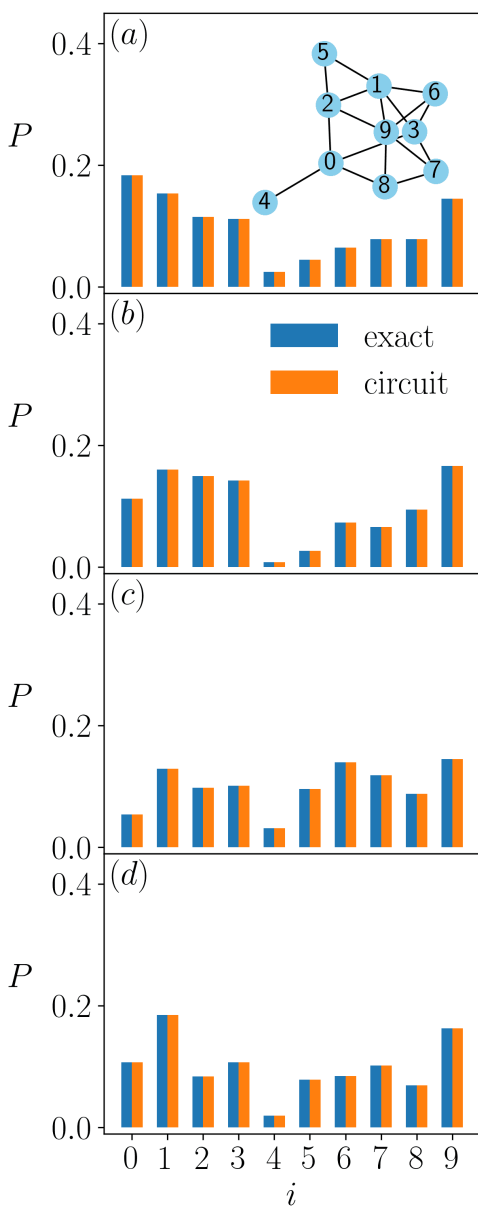


Figure 3. The probability histogram of quantum walk on Erdős-Rényi random graph with  $n = 10$  nodes and edge probability  $p = 0.3$ . The exact and circuit in the legend represent the exact value and simulation value by the state vector simulator for the quantum walk algorithm, respectively. (a)  $t = 1$  (b)  $t = 2$  (c)  $t = 3$  and (d)  $t = 4$ .

	Previous work [27]	Proposed method
Circuit width	$\lceil \log_2 N \rceil + \lceil \log_2  E  \rceil$	$2 \lceil \log_2 N \rceil$
Coin operator	$\mathcal{O}(N)$	$\mathcal{O}(N)$
Shift operator	$\mathcal{O}( E  \cdot \text{poly}(\log N))$	$\mathcal{O}(\log N)$

Table II. Comparison of resource requirements. The table lists the required number of qubits (Circuit width) and the gate complexity for the coin and shift operators.

result suggests that the proposed method is robust to topological variations in complex networks. The scaling exponent of  $\approx 1.9$  indicates that the circuit complexity is mainly determined by the state preparation  $\hat{U}_2$  or node-dependent coin operators  $\hat{C}_i$ . While the

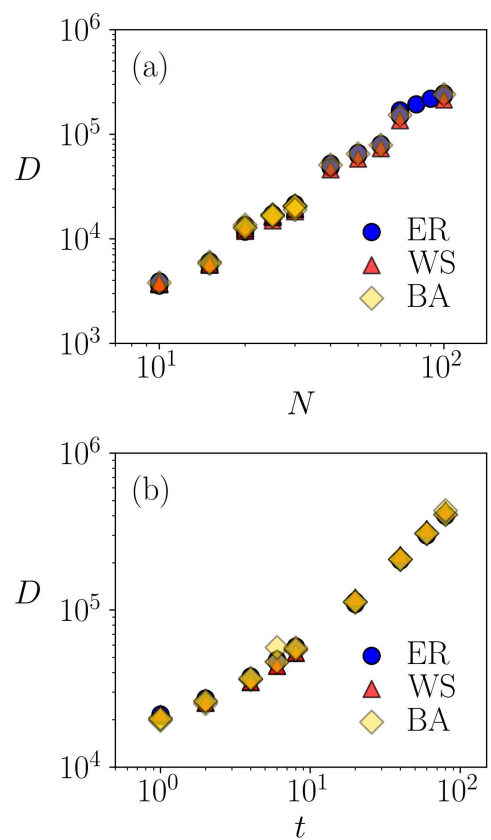


Figure 4. (a) The node-dependent depths of coined quantum walk circuits for the ER model, WS model, and BA model. The circuits are evaluated at time step  $t = 1$ . (b) The time-dependent depths of coined quantum walk circuits for the ER model, WS model, and BA model. The circuits are evaluated for  $N = 2^5$ .

standard Grover walk on regular graphs can be implemented with fewer resources, the quantum walk on arbitrary complex networks requires the polynomial gate complexity.

We compare the resource requirements of our previous approach [27]. The previous method required  $\lceil \log_2 N \rceil + \lceil \log_2 |E| \rceil$  qubits because it encodes both node and edge information. In contrast, our new approach requires the width of our circuit is given by  $2 \lceil \log_2 N \rceil$ , as we use two registers proportional to  $N$  for encoding node information and coin state. For the three models in this study, the number of edges  $E$  is equal to or greater than the number of nodes  $N$  ( $|E| \geq N$ ), and realizes a more efficient resource. This means the proposed circuit can be implemented using fewer qubits than previous approaches in all cases.

Second, the proposed method significantly reduces the total number of gates. In earlier methods, the shift operation relied on up to  $|E|$  multi-controlled X (MCX) gates. Since an MCX gate requires more CNOTs as the number of control qubits increases, the total CNOT count scales approximately as  $\mathcal{O}(|E| \cdot \text{poly}(\log N))$ . In contrast, the proposed circuit employs SWAP gates for the shift operation, requiring a count proportional to  $\lceil \log_2 N \rceil$ . Since each of these gates decomposes into three CNOTs, the total complexity becomes  $3 \times \lceil \log_2 N \rceil = \mathcal{O}(\log N)$ . This leads

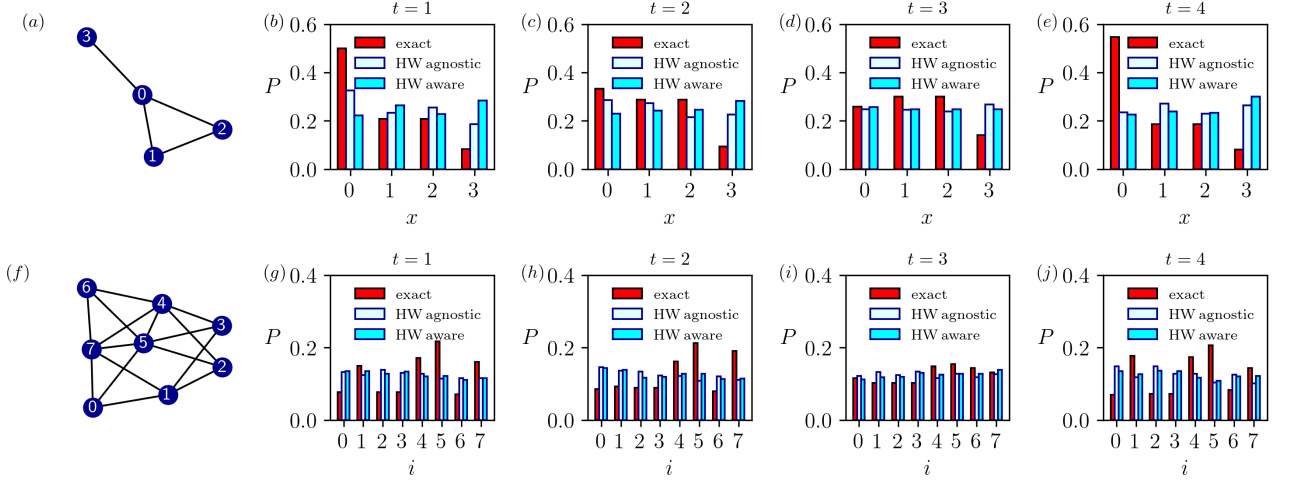


Figure 5. Time-evolution of the probability distribution for a quantum walk on two different WS models. The histograms compare the exact theoretical simulation (red bars) with experimental results obtained from the `ibm_torino` backend (10000 shots). The experimental data contrast hardware (HW) agnostic (dark blue outline) and HW-aware (cyan filled) synthesis strategies. (a) A WS model with  $N = 4$ ,  $k = 2$ , and  $\beta = 0.2$ . (b)–(e) Probability distributions at time steps  $t = 1$  to  $t = 4$  for the graph in (a). (f) A WS model with  $N = 8$ ,  $k = 2$ , and  $\beta = 0.2$ . (g)–(j) Corresponding probability distributions for time steps  $t = 1$  to  $t = 4$ .

to a major reduction in resources, especially for dense complex networks.

We also validated the feasibility of our approach using `ibm_torino`. The experimental results showed that the impact of hardware-aware optimization varies depending on the graph scale. For the  $N = 8$  graph, the hardware-aware synthesis reduced the circuit depth and improved the  $L_1$  distance. In contrast, for the  $N = 4$  smaller graph, the overhead from qubit connectivity constraints became significant and outweighed the benefits of optimization. This indicates that while the proposed circuit is scalable in theory, the limited connectivity of current NISQ devices remains a challenge. Therefore, topology-aware circuit design becomes increasingly critical as the graph size and circuit complexity increase.

Finally, we discuss the hardware requirements for practical applications. Based on the scaling law  $D \approx 40N^{1.9}$  derived from our results, implementing the coined quantum walk on a network of size  $N = 100$  requires a circuit depth of approximately  $2.5 \times 10^5$ . This depth exceeds the capacity of current NISQ devices and implies a per-gate error threshold of  $\epsilon \sim 10^{-5}$ . This threshold is derived from the standard approximation that the total error probability,  $\epsilon \times D$ , must remain below unity for meaningful computation [35]. Since state-of-the-art physical qubits typically exhibit error rates around  $10^{-3}$  to  $10^{-4}$  [36], executing such deep circuits ( $D \sim 10^5$ ) is infeasible on NISQ devices and requires the use of logical qubits.

## VII. CONCLUSIONS

In this work, we proposed a programmable quantum circuit framework for coined discrete-time quantum walks on complex networks. The design is based on a dual-register encoding that enables localized coin operations and a shift operator implemented via SWAP gates. This circuit design significantly reduces the resource overhead compared to previous edge-encoding methods, making it suitable for graphs with arbitrary degree distributions. We demonstrated the robustness of the design through simulation across Erdős–R’enyi, Watts–Strogatz, and Barab’asi–Albert models. The circuit depth scales polynomially, approximately as  $N^{1.9}$ , indicating consistent scaling behavior regardless of the network topology. Furthermore, we confirmed the practical feasibility of our approach by synthesizing and executing the circuits on the `ibm_torino` superconducting quantum processor. The experimental results showed that the effectiveness of hardware-aware optimization depends on the graph scale. Although connectivity constraints caused overhead for small graphs, the optimization reduced the circuit depth for larger graphs. This suggests that topology-aware circuit design becomes important as the graph size increases. Our framework provides a flexible tool for investigating quantum dynamics on graph-structured data. Based on our scaling analysis, current NISQ devices are limited to small-scale validations. However, practical applications of quantum walks on medium-sized networks are expected to become feasible in the early fault-tolerant quantum computing era.

[2] David Orrell. A quantum walk model of financial options. *Wilmott*, 2021(112):62–69, 2021.

[3] Pablo Antonio Moreno Casares, Roberto Campos, and Miguel Angel Martin-Delgado. Qfold: quantum walks and deep learning to solve protein folding. *Quantum Science and Technology*, 7(2):025013, 2022.

[4] Andrew M. Childs and Jeffrey Goldstone. Spatial search by quantum walk. *Phys. Rev. A*, 70:022314, Aug 2004.

[5] Y. Aharonov, L. Davidovich, and N. Zagury. Quantum random walks. *Phys. Rev. A*, 48:1687–1690, Aug 1993.

[6] M. Szegedy. Quantum speed-up of markov chain based algorithms. In *45th Annual IEEE Symposium on Foundations of Computer Science*, pages 32–41, 2004.

[7] Andris Ambainis, Julia Kempe, and Alexander Rivosh. Coins make quantum walks faster. In *Proceedings of the Sixteenth Annual ACM-SIAM Symposium on Discrete Algorithms*, SODA '05, page 1099–1108, USA, 2005. Society for Industrial and Applied Mathematics.

[8] Rei Sato, Tetsuro Nikuni, Kayoko Nohara, Giorgio Salani, and Shohei Watabe. Universal scaling hypothesis of quantum spatial search in complex networks. *Phys. Rev. Res.*, 6:043119, Nov 2024.

[9] Prateek Chawla, Roopesh Mangal, and C Madaiah Chandrashekhar. Discrete-time quantum walk algorithm for ranking nodes on a network. *Quantum Information Processing*, 19:1–21, 2020.

[10] Giuseppe Davide Paparo, Markus Müller, Francesc Comellas, and Miguel Angel Martin-Delgado. Quantum google in a complex network. *Scientific reports*, 3(1):2773, 2013.

[11] Stefan Dernbach, Arman Mohseni-Kabir, Siddharth Pal, Miles Gepner, and Don Towsley. Quantum walk neural networks with feature dependent coins. *Applied Network Science*, 4:1–16, 2019.

[12] Xinyu Ye, Ge Yan, and Junchi Yan. Vqne: Variational quantum network embedding with application to network alignment. In *Proceedings of the 29th ACM SIGKDD Conference on Knowledge Discovery and Data Mining*, pages 3105–3115, 2023.

[13] Rei Sato, Shuichiro Haruta, Kazuhiro Saito, and Mori Kurokawa. Qwalkvec: Node embedding by quantum walk. In *Pacific-Asia Conference on Knowledge Discovery and Data Mining*, pages 93–104. Springer, 2024.

[14] Anurag Singh and Binshumesh Sachan. A quantum approach to walk on networks. In *2021 6th International Conference on Signal Processing, Computing and Control (ISPCC)*, pages 636–643. IEEE, 2021.

[15] Jigjen Bhavsar, Shashank Shekhar, and Siddhartha Santra. Coined quantum walk on a quantum network. *Physical Review A*, 110(5):052428, 2024.

[16] C Huerta Alderete, Shivani Singh, Nhung H Nguyen, Daiwei Zhu, Radhakrishnan Balu, Christopher Monroe, CM Chandrashekhar, and Norbert M Linke. Quantum walks and dirac cellular automata on a programmable trapped-ion quantum computer. *Nature communications*, 11(1):3720, 2020.

[17] Frank Acasiete, Flavia P Agostini, J Khatibi Moqadam, and Renato Portugal. Implementation of quantum walks on ibm quantum computers. *Quantum Information Processing*, 19:1–20, 2020.

[18] Allan Wing-Bocanegra and Salvador E Venegas-Andraca. Circuit implementation of discrete-time quantum walks via the shunt decomposition method. *Quantum Information Processing*, 22(3):146, 2023.

[19] Allan Wing-Bocanegra, Carlos E Quintero-Narvaez, and Salvador E Venegas-Andraca. Circuit implementation and analysis of a quantum-walk based search complement algorithm. *Scientific Reports*, 15(1):4865, 2025.

[20] Luca Razzoli, Gabriele Cenedese, Maria Bondani, and Giuliano Benenti. Efficient implementation of discrete-time quantum walks on quantum computers. *Entropy*, 26(4):313, 2024.

[21] T Loke and JB Wang. Efficient circuit implementation of quantum walks on non-degree-regular graphs. *Physical Review A*, 86(4):042338, 2012.

[22] Thomas Loke and Jingbo B Wang. Efficient quantum circuits for continuous-time quantum walks on composite graphs. *Journal of Physics A: Mathematical and Theoretical*, 50(5):055303, 2017.

[23] Ugo Nzongani, Julien Zylberman, Carlo-Elia Doncicchi, Armando Pérez, Fabrice Debbasch, and Pablo Arnaudt. Quantum circuits for discrete-time quantum walks with position-dependent coin operator. *Quantum Information Processing*, 22(7):270, 2023.

[24] Renato Portugal and Jalil Khatibi Moqadam. Efficient circuit implementations of continuous-time quantum walks for quantum search. *Entropy*, 27(5):454, 2025.

[25] Sabyasachi Chakraborty, Rohit Sarma Sarkar, Sonjoy Majumder, and Rohit Kishan Ray. Continuous-time quantum walk on a random graph using quantum circuits. *arXiv preprint arXiv:2510.14905*, 2025.

[26] Zhaoyang Chen, Guanzhong Li, and Lvzhou Li. Implementation of a continuous-time quantum walk on a sparse graph. *Phys. Rev. A*, 110:052215, Nov 2024.

[27] Rei Sato and Kazuhiro Saito. Circuit Implementation of Discrete-Time Quantum Walks on Complex Networks . In *2024 IEEE International Conference on Quantum Computing and Engineering (QCE)*, pages 376–377, Los Alamitos, CA, USA, September 2024. IEEE Computer Society.

[28] Duncan J Watts and Steven H Strogatz. Collective dynamics of ‘small-world’networks. *nature*, 393(6684):440–442, 1998.

[29] Albert-László Barabási and Réka Albert. Emergence of scaling in random networks. *science*, 286(5439):509–512, 1999.

[30] P ERDdS and A R&wi. On random graphs i. *Publ. math. debrecen*, 6(290-297):18, 1959.

[31] Matan Vax, Peleg Emanuel, Eyal Cornfeld, Israel Reichental, Ori Opher, Ori Roth, Tal Michaeli, Lior Premlinger, Lior Gazit, Amir Naveh, et al. Qmod: Expressive high-level quantum modeling. *arXiv preprint arXiv:2502.19368*, 2025.

[32] Tomer Goldfriend, Israel Reichental, Amir Naveh, Lior Gazit, Nadav Yoran, Ravid Alon, Shmuel Ur, Shahak Lahav, Eyal Cornfeld, Avi Elazari, et al. Design and synthesis of scalable quantum programs. *arXiv preprint arXiv:2412.07372*, 2024.

[33] Salvador Elías Venegas-Andraca. Quantum walks: a comprehensive review. *Quantum Information Processing*, 11(5):1015–1106, 2012.

[34] Classiq Technologies. Hardware-aware synthesis. <https://docs.classiq.io/latest/user-guide/synthesis/hardware-aware-synthesis/>, 2024. Accessed on 15.11.2025.

[35] Michael A Nielsen and Isaac L Chuang. *Quantum computation and quantum information*. Cambridge university press, 2010.

[36] Google Quantum AI. Suppressing quantum errors by scaling a surface code logical qubit. *Nature*, 614(7949):676–681, 2023.

## Supplemental Material for "Coined Quantum Walks on Complex Networks for Quantum Computers"

### Appendix A: Implementation with Qmod

Here, we provide a step-by-step explanation of the Qmod implementation corresponding to the mathematical model of the coined quantum walk described in the main text. The implementation leverages Qmod's high-level abstractions to automatically synthesize circuits for arbitrary complex networks.

First, we define the complex network structure using `networkx`. For this example, we generate a Watts-Strogatz graph. We also prepare helper functions to extract node degrees and neighbor information, which correspond to the adjacency matrix elements  $A_{i,j}$  and degree  $k_i$  in the theoretical model.

---

```
from classiq import *
import numpy as np
import networkx as nx

N = 8
k = 2
beta = 0.5
G = nx.watts_strogatz_graph(N, k, beta)
num_qubits = int(np.ceil(np.log2(N)))

def get_edges_of_node(G, i):
    return [j for j in G.neighbors(i)]

def inner_degree(G, i):
    """
    Constructs the probability distribution for the neighbor states of node i.
    This corresponds to the uniform superposition over neighbors in Eq. (3).
    """
    l_array = np.zeros(2**num_qubits)
    neighbors_list = get_edges_of_node(G, i)
    k = len(neighbors_list)
    for j in neighbors_list:
        l_array[j] = 1
    # Normalized probability for state preparation
    return l_array / k
```

---

#### 1. State Preparation

The preparation of the state involves two steps. The operator  $\hat{U}_1$  creates a uniform superposition over all nodes in the first register `x` (representing node  $i$ ).

$$\hat{U}_1 |0\rangle^n = \frac{1}{\sqrt{N}} \sum_{i=0}^{N-1} |i\rangle \quad (\text{A1})$$

In Qmod, if  $N$  is a power of 2, this is a simple Hadamard transform. Otherwise, we use `inplace_prepare_state` with a uniform probability distribution.

The operator  $\hat{U}_2^{(i)}$  prepares the coin state with a superposition of neighbors for a specific node  $i$  in the second register `y` (representing neighbor  $j$ ).

$$\hat{U}_2^{(i)} |0\rangle^n = \frac{1}{\sqrt{k_i}} \sum_{j=0}^{N-1} A_{i,j} |j\rangle \quad (\text{A2})$$

This is implemented using a `control` block iterating over all nodes  $i$ . For each  $i$ , the target operation `inplace_prepare_state` initializes register `y` based on the local connectivity defined by `inner_degree(G, i)`.

---

```
@qfunc
def prepare_initial_state(x: QNum[num_qubits], y: QNum[num_qubits]):
    # Implementation of U1 on register x
```

```

if N == 2**num_qubits:
    hadamard_transform(x)
else:
    prob_array = np.ones(2**num_qubits) / N
    prob_array[N:2**num_qubits] = 0
    inplace_prepare_state(prob_array.tolist(), 0.0, x)

# Implementation of controlled-U2 on register y
for i in range(N):
    control(
        x == i,
        lambda: inplace_prepare_state(inner_degree(G, i).tolist(), 0.0, y),
    )

```

## 2. Coin Operator

The coin operator  $\hat{C}$  applies a local Grover diffusion operator at each node. Mathematically, for each node  $i$ , the local coin  $\hat{C}_i$  is:

$$\hat{C}_i = 2\hat{U}_2^{(i)} |0\rangle\langle 0| (\hat{U}_2^{(i)})^\dagger - \hat{I} \quad (\text{A3})$$

In Qmod, the `grover_diffuser` function automatically implements the reflection  $2|s\rangle\langle s| - I$  given a state preparation oracle. Here, the oracle is exactly the `inplace_prepare_state` function used for  $\hat{U}_2^{(i)}$ . We wrap this in a `control` block to apply the specific diffuser for each node position  $i$  (corresponding to register `x`).

```

@qfunc
def my_coin(x: QNum[num_qubits], y: QNum[num_qubits]):
    for i in range(N):
        control(
            x == i,
            stmt_block=lambda: grover_diffuser(
                lambda y: inplace_prepare_state(inner_degree(G, i).tolist(), 0.0, y),
                y
            )
        )

```

## 3. Shift Operator

The shift operator performs a flip-flop shift by swapping the position and direction registers.

$$\hat{S} |i\rangle |j\rangle = |j\rangle |i\rangle \quad (\text{A4})$$

This corresponds to a swap of the two quantum registers `x` and `y`. In Qmod, this is concisely expressed using the `multiswap` gate.

```

@qfunc
def my_shift(x: QNum[num_qubits], y: QNum[num_qubits]):
    multiswap(x, y)

```

## 4. Whole Circuit

Finally, the discrete-time quantum walk is constructed by iteratively applying the coin and shift operators. The `power` function in Qmod efficiently implements the repetition of the step unitary  $U^t = (\hat{S}\hat{C})^t$ .

```

@qfunc
def discrete_quantum_walk(
    time: CInt,
    coin_qfuncs: QCallable[QNum, QNum],
    shift_qfuncs: QCallable[QNum, QNum],
    x: QNum,
    y: QNum
):
    power(
        time,

```

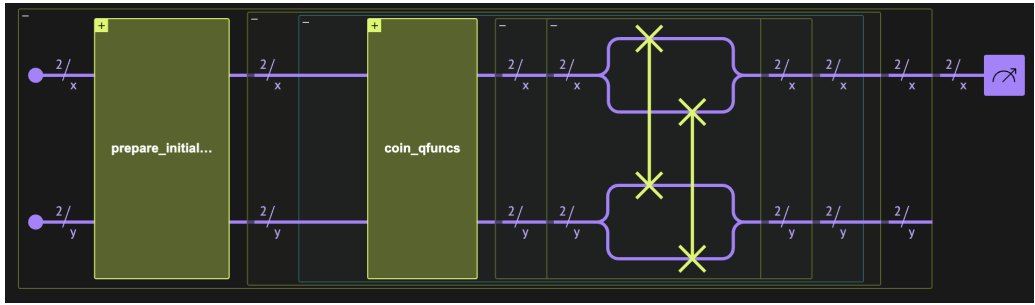


Figure 6. Quantum circuit for the coined quantum walk synthesized using the Classiq Platform. The circuit implements the walk dynamics on a complex network with  $N = 4$  nodes. The first and second blocks represent the initial state preparation and the coin operator, respectively. The `swap_gate` block corresponds to the flip-flop shift operator.

```

        lambda: (
            coin_qfuncs(x, y),
            shift_qfuncs(x, y),
        ),
    )

@qfunc
def main(x: Output[QNum[num_qubits]]):
    y = QNum("y", num_qubits)
    allocate(num_qubits, x)
    allocate(num_qubits, y)

    # Initialize state |psi(0)>
    prepare_initial_state(x, y)

    # Execute walk for t=1 step
    discrete_quantum_walk(1, my_coin, my_shift, x, y)

```

## 5. Circuit Synthesis

We employ two distinct synthesis strategies to generate the final quantum circuits: hardware-agnostic synthesis for simulation and hardware-aware synthesis for execution on real devices.

For numerical simulations and logical verification, we generate the circuit without targeting a specific backend. This approach optimizes for general logical depth and qubit count, independent of physical constraints.

```

# Standard Synthesis
qmod = create_model(main)
qprog = synthesize(qmod)

```

For the experimental validation on the `ibm_torino` processor, we utilize hardware-aware synthesis. By defining a `Preferences` object with the specific backend provider and name, the synthesis engine optimizes the gate decomposition and routing to match the device's connectivity and basis gate set. This step is crucial for minimizing the error rates discussed in the experimental results.

```

# Hardware-aware Synthesis
preferences = Preferences(
    backend_service_provider="IBM Quantum",
    backend_name="ibm_torino"
)

# Synthesize with hardware constraints
qmod_hw = create_model(main, preferences=preferences)
qprog_hw = synthesize(qmod_hw)

```

## 6. Visualization

Finally, Qmod provides built-in tools to visualize the synthesized quantum circuit and analyze its properties. The `show()` function opens an interactive circuit viewer, allowing for a hierarchical inspection of the block-encoded operators, as shown in Fig. 6. This command generates the quantum circuit diagrams presented in

the main text, confirming that the high-level functional definitions are correctly compiled into the gate-level implementation.

---

```
# Visualize the generated circuit
show(qprog)

# (Optional) Analyze circuit properties such as depth
# print(qprog.transpiled_circuit.depth)
```

---